

# Facultative and anaerobic consortia of haloalkaliphilic ureolytic micro-organisms capable of precipitating calcium carbonate

D. J. Skorupa, A. Akyel, M. W. Fields, R. Gerlach

This is the peer reviewed version of the following article: [Skorupa, D.J., Akyel, A., Fields, M.W., and Gerlach, R. (2019). Facultative and anaerobic consortia of haloalkaliphilic ureolytic micro-organisms capable of precipitating calcium carbonate. *Journal of Applied Microbiology* 127, 1479–1489.], which has been published in final form at <https://doi.org/10.1111/jam.14384>. This article may be used for non-commercial purposes in accordance with Wiley Terms and Conditions for Use of Self-Archived Versions.

Skorupa, D.J., Akyel, A., Fields, M.W., and Gerlach, R. (2019). Facultative and anaerobic consortia of haloalkaliphilic ureolytic micro-organisms capable of precipitating calcium carbonate. *Journal of Applied Microbiology* 127, 1479–1489 <https://doi.org/10.1111/jam.14384>

<https://creativecommons.org/licenses/by-nc-nd/4.0/>



1 Facultative and anaerobic consortia of haloalkaliphilic ureolytic  
2 microorganisms capable of precipitating calcium carbonate

3 **Dana J. Skorupa<sup>1,2</sup>, Arda Akyel<sup>1,2</sup>, Matthew W. Fields<sup>2,3</sup>, and Robin**  
4 **Gerlach<sup>1,2†</sup>**

5  
6 *<sup>1</sup>Department of Chemical and Biological Engineering, Montana State University, Bozeman, MT,*  
7 *59717, USA*

8 *<sup>2</sup>Center for Biofilm Engineering, Montana State University, Bozeman, MT, 59717, USA*

9 *<sup>3</sup>Department of Microbiology and Immunology, Montana State University, Bozeman, MT, 59717,*  
10 *USA*

11  
12 **Abbreviated Running Headline:** Facultative and anaerobic MICP

13  
14 † Corresponding author: Robin Gerlach, Montana State University, 59717-3980, PO Box  
15 173920, Room 314 Cobleigh Hall, Bozeman, MT, USA.

16 E-mail: robin\_g@montana.edu  
17  
18  
19  
20  
21  
22  
23

24 **Abstract**

25 **Aims:** Development of biomineralization technologies has largely focused on microbially induced  
26 carbonate precipitation (MICP) via *Sporosarcina pasteurii* ureolysis; however, as an obligate  
27 aerobe, the general utility of this organism is limited. Here, facultative and anaerobic  
28 haloalkaliphiles capable of ureolysis were enriched, identified and then compared to *S. pasteurii*  
29 regarding biomineralization activities.

30 **Methods and Results:** Anaerobic and facultative enrichments for haloalkaliphilic and ureolytic  
31 microorganisms were established from sediment slurries collected at Soap Lake (WA). Optimal  
32 pH, temperature, and salinity were determined for highly ureolytic enrichments, with dominant  
33 populations identified via a combination of high-throughput SSU rRNA gene sequencing, clone  
34 libraries, and Sanger sequencing of isolates. The enrichment cultures consisted primarily of  
35 *Sporosarcina*- and *Clostridium*-like organisms. Ureolysis rates and direct cell counts in the  
36 enrichment cultures were comparable to the *S. pasteurii* (strain ATCC 11859) type strain.

37 **Conclusions:** Ureolysis rates from both facultatively and anaerobically enriched  
38 haloalkaliphiles were either not statistically significantly different to, or statistically significantly  
39 higher than, the *S. pasteurii* (strain ATCC 11859) rates. Work here concludes that extreme  
40 environments can harbor highly ureolytic active bacteria with potential advantages for large scale  
41 applications, such as environments devoid of oxygen.

42 **Significance and Impact of the Study:** The bacterial consortia and isolates obtained add to  
43 the possible suite of organisms available for MICP implementation, therefore potentially  
44 improving the economics and efficiency of commercial biomineralization.

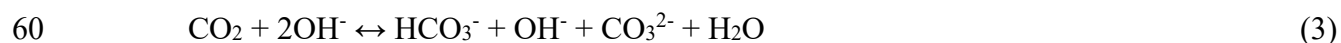
45

46 **Keywords** biomineralization, bio-inventory, haloalkaliphile, ureolysis activity, calcium  
47 carbonate.

48

## 49 **Introduction**

50 Biomineralization is the generation of minerals by living organisms. Mineral precipitation can  
51 occur either directly or indirectly, with indirect synthesis arising when intracellular metabolic  
52 activities within a cell result in extracellular supersaturation and mineral precipitation. The best  
53 studied example of indirect mineral production likely is microbially induced calcium carbonate  
54 precipitation (MICP), where the microbially-driven hydrolysis of urea results in the production of  
55 ammonia (NH<sub>3</sub>) and dissolved inorganic carbon (DIC) (eq 1). The reaction increases pH and  
56 carbonate alkalinity (eq 2 and 3) and favors the precipitation of CaCO<sub>3</sub> when dissolved calcium is  
57 present (eq 4; Lauchnor et al., 2013).



62 The process is applicable to numerous engineered applications, from carbon sequestration  
63 (Mitchell et al., 2010) and groundwater remediation (Achal et al., 2012), to soil stabilization  
64 (Whiffin et al., 2007) and improved subsurface barriers (Rusu et al., 2011). The most common  
65 organism used in subsurface engineered biomineralization applications is the ureolytic bacterium  
66 *Sporosarcina pasteurii* (Phillips et al., 2013). By injecting this organism into the subsurface in  
67 combination with a supply of dissolved calcium and urea, the precipitation of calcium carbonate  
68 (CaCO<sub>3</sub>) in the surrounding environment, allows for small leaks in porous rock formations to be  
69 sealed or porous media, such as soils, to be stabilized. *S. pasteurii* produces significant amounts

70 of urease (Ferris et al., 1996; Stocks-Fisher et al., 1999; DeJong et al., 2006) and is effective at  
71 mineralization across a variety of size scales (*e.g.*, summarized in Phillips et al., 2013; Phillips et  
72 al., 2016). However, the long-term use of tested laboratory strains under field-relevant conditions  
73 and their tolerance to the pressures, temperatures, salt concentrations, and oxygen conditions  
74 observed in the deeper subsurface is a challenge (Martin et al., 2012; Martin et al., 2013).

75         Recent work has shown *S. pasteurii* to be incapable of growth in the absence of oxygen  
76 (Martin et al., 2012), indicating that repeated injections of the organism would be required to  
77 maintain long term biomineralization in anoxic subsurface environments. As well, though *S.*  
78 *pasteurii* is capable of growth in sea water (Mortensen et al., 2011), deep aquifers can contain  
79 significantly higher salinity levels (Bassett and Bentley, 1983) potentially resulting in urease  
80 inhibition. Urease activity is also known to be pH-dependent, with a pH of approximately 7 being  
81 described as optimal for known enzymes (Fidaleo and Lavecchia, 2003). This pH dependence  
82 could inhibit the biological activity of organisms like *S. pasteurii* in the subsurface because water  
83 associated with well cement can routinely have pH values between 11 and 13 (Bang et al. 2001;  
84 Jonkers et al. 2010). These limitations with *S. pasteurii* create a need to isolate alternative  
85 microorganisms adapted to the extreme conditions potentially encountered in the deep subsurface.

86         This study examines the ability of haloalkaliphilic organisms to perform ureolysis-induced  
87 CaCO<sub>3</sub> precipitation under either (initially) low-oxygen (‘facultative’) or anaerobic conditions.  
88 The primary objectives were (1) to enrich urea-hydrolyzing microorganisms naturally adapted to  
89 high salinity, alkaline, and anoxic environments, thus selecting for ureolytic organisms adapted to  
90 conditions likely to be encountered in deep sub-surface rock formations; (2) identify the dominant  
91 microbial populations and morphologies using DNA sequencing and microscopy; and (3) compare

92 the ureolytic activity of haloalkaliphilic enrichment cultures to the current MICP model organism,  
93 *S. pasteurii*.

94

## 95 **Materials and Methods**

### 96 *Site Description, aqueous chemical analyses, and biomass collection*

97 Sediment slurry samples were collected for microbial enrichments from three different locations  
98 within or adjacent to Soap Lake, a meromictic, alkaline, saline lake located in central Washington,  
99 USA. Sampling was conducted in January 2015 at locations identified as SL2 (47.24340 N,  
100 119.29412 W), SL3 (47.31394 N, 119.29594 W), and SL4 (47.30770 N, 119.30006 W). Biomass  
101 was collected by aseptically gathering a soil and/or sediment slurry and transferring it into a sterile  
102 50 mL conical tube. Following collection, samples were maintained at 4°C until cultures could be  
103 established. The temperature, pH, and electrical conductivity of each site was measured *in situ*  
104 using a combined pH-temperature probe and meter-compatible electrical conductivity probe (YSI  
105 Incorporated, Yellow Springs, OH).

106 Aqueous geochemistry was also assessed at sites SL2 and SL3; the sample from site SL4  
107 consisted of solid material only (top soil from a salt flat) and therefore no aqueous geochemistry  
108 data are available. Briefly, site water was filter-sterilized (0.22 µm) directly into sterile 50 mL  
109 conical tubes. Some filtered site water was acidified in the field with 5% trace metal grade nitric  
110 acid prior to transport and used for total dissolved metals analysis. Concentrations of total metals  
111 were measured using an Agilent 7500ce ICP-MS by comparing to certified standards (Agilent  
112 Technologies, Environmental Calibration Standard 5183-4688). Ion chromatography was used to  
113 determine concentrations of dominant anions. For this, non-acidified filtered samples were  
114 analyzed using a Dionex ICS-1100 chromatography System (Dionex Corp., Sunnyvale, CA)

115 equipped with a 25  $\mu\text{L}$  injection loop and an AS22-4x250 mm anion exchange column, using an  
116 eluent concentration of 4.5  $\text{mmol l}^{-1}$  sodium carbonate and 1.4  $\text{mmol l}^{-1}$  sodium bicarbonate  
117 flowing at a rate of 1.2  $\text{mL}\cdot\text{min}^{-1}$ . An overview of the aqueous geochemistry is given in Table S1;  
118 the following were not detected  $\text{NO}_2^-$ ,  $\text{Br}^-$ ,  $\text{PO}_4^{3-}$ , and dissolved Fe.

119 Samples were also collected for total community analysis by filtering 2 L of site water from  
120 each sampling location through a 0.22  $\mu\text{m}$  filter. The filters were aseptically transferred into a 50  
121 mL conical vial, immediately placed on dry ice, and stored at  $-80^\circ\text{C}$  until DNA extraction.

#### 122 *Enrichment, Optimal Growth Conditions, and Microbially-Induced $\text{CaCO}_3$ Precipitation Activity*

123 Calcium mineralizing medium (CMM) was used to enrich ureolytic bacteria. The medium  
124 consisted of 3  $\text{g l}^{-1}$  Difco Nutrient Broth (BD, Sparks MD), 333  $\text{mmol l}^{-1}$  urea, 187  $\text{mmol l}^{-1}$   
125  $\text{NH}_4\text{Cl}$ , and was modified with both 0.077  $\text{mmol l}^{-1}$   $\text{NiCl}_2$  and 50  $\text{g l}^{-1}$   $\text{NaCl}$ . The medium was  
126 prepared either anaerobically ( $\text{N}_2$  headspace) or aerobically, pH adjusted to 9 with 5  $\text{mol l}^{-1}$   $\text{NaOH}$ ,  
127 distributed into 30 mL Hungate tubes sealed with butyl-rubber stoppers, and sterilized by  
128 autoclaving. Enrichment cultures were established in triplicate by inoculating Hungate tubes  
129 containing 9 mL of autoclaved CMM medium with 1 mL of environmental sediment slurry (10%  
130 [vol·vol $^{-1}$ ]) and incubation at  $37^\circ\text{C}$  without shaking. Enrichments were screened for ureolytic  
131 activity by monitoring urea concentrations in filtered (0.22  $\mu\text{m}$  filter) subsamples using a modified  
132 Jung assay (Jung et al., 1975; Phillips et al., 2016). Enrichment cultures positive for ureolysis were  
133 transferred into fresh medium for continued cultivation.

134 Subsequent experiments investigating  $\text{CaCO}_3$  precipitation efficacy used CMM medium  
135 with the pH adjusted to 6 prior to autoclaving. The medium was amended with 33  $\text{mmol l}^{-1}$   
136 sterilized  $\text{CaCl}_2\cdot 2\text{H}_2\text{O}$  prior to inoculation with 10% [vol·vol $^{-1}$ ] of culture before static incubation  
137 at  $30^\circ\text{C}$ . Liquid samples were collected every two hours, passed through a 0.22  $\mu\text{m}$  filter and

138 analyzed for pH and dissolved concentrations of urea using a modified Jung assay (Jung et al.,  
139 1975; Philips, 2013a). Dissolved levels of  $\text{Ca}^{2+}$  were measured using filtered samples and were  
140 determined via spectrophotometry measurements at 620 nm using a modified calcium-*o*-  
141 cresolphthalein complexome method (Kanagasabapathy and Kumari, 2000). Alkalinity was  
142 tracked after diluting samples (1:50) in water (18.2 M $\Omega$ .cm) and titrating with HCl (0.1 mol l<sup>-1</sup>) to  
143 a pH of 4.5 using an automatic titrator (HI 902, Hanna Instruments, Woonsocket, RI). Mineral  
144 precipitates were dried and characterized at the end of the experiment using a LabRAM HR  
145 Evolution Confocal Raman microscope (Horiba Scientific, France) at 100-500x magnification and  
146 a 532 nm laser (100 mW). Spectra were collected over a 100-2000 cm<sup>-1</sup> range using an 1800 gr/mm  
147 grating and a 1024 x 256 pixel air cooled CCD detector. Peak identification was supported using  
148 the KnowItAll Raman spectra library (Bio-Rad, Hercules, CA).

149 CMM medium was also utilized to determine the optimal temperature, pH and salt  
150 concentrations for established ureolytic enrichments. Cultures were incubated at 20, 25, 30, 37,  
151 40, and 45°C without shaking to determine the optimal growth temperature. After determining the  
152 optimal growth temperature, the effects of pH on growth were monitored by poisoning the pH at  
153 values ranging from 6.0 to 11.0 using either NaOH or HCl. Finally, optimal salt concentrations  
154 were determined by varying NaCl levels between no addition and 4.3 mol l<sup>-1</sup> using the optimal  
155 growth temperature and pH value. Treatments were monitored for growth by collecting optical  
156 density measurements at 600 nm (Unico, S-1100 VIS spectrophotometer, 1 cm path length).  
157 Identical physiological tests were also conducted on a pure culture of the model MICP strain *S.*  
158 *pasteurii* (ATCC 11859) during growth in Brain Heart Infusion (BHI) medium (Becton  
159 Dickinson).

160 Urea hydrolysis kinetics of haloalkaliphilic enrichment cultures were compared to those of  
161 the model MICP strain *S. pasteurii* (strain ATCC 11859) using CMM containing 333 mmol l<sup>-1</sup>  
162 urea. CMM was inoculated with a 10% [vol·vol<sup>-1</sup>] culture volume, and urea concentrations were  
163 tracked using the modified Jung assay described above. Changes in total cell numbers were  
164 monitored using acridine orange staining and direct cell counting. Briefly, 1.98 mL of sample was  
165 mixed with 20 µl acridine orange (40 mg·mL<sup>-1</sup>) and incubated at room temperature for 30 minutes  
166 before rinsing with nanopure water. The stained sample was filtered onto a black polycarbonate  
167 0.22 µm membrane filter, washed with nanopure water, dried and mounted on a microscope slide  
168 using immersion oil. Slides were viewed using a transmitted/epifluorescence light microscope  
169 (Nikon Eclipse E800) with an Infinity 2 color camera with the appropriate filter set. A total of 10-  
170 30 microscopy fields were counted for each sample slide.

#### 171 *DNA extraction, PCR, and sequencing*

172 DNA for total community analysis was extracted from each collected Soap Lake filter using a  
173 modified version of the FastDNA Spin Kit for Soil (MP Biomedicals, Solon, OH). Frozen filters  
174 were aseptically cut in half, with one half placed in a sterile petri dish for DNA extraction. Unused  
175 sections of the filter were stored at -80°C. The half filter was further cut into smaller pieces and  
176 aseptically transferred to a Lysing Matrix E tube. DNA was also extracted from facultative and  
177 anaerobic ureolytic enrichments to identify cultivated species. Briefly, 30 mL of enrichment  
178 culture was harvested by centrifugation, the pellet re-suspended in the provided MP Biomedicals  
179 phosphate buffer and transferred to a Lysing Matrix E tube. The DNA extraction for both the filters  
180 and enrichment sample types then continued according to the manufacturer's instructions.  
181 Following extraction, the DNA from the filter and enrichment samples was cleaned and  
182 concentrated using a OneStep<sup>TM</sup> PCR Inhibitor Removal Kit (Zymo Research, Irvine, CA) and

183 Qiaquick PCR Purification Kit (Qiagen, Valencia, CA). DNA extraction from axenic isolates  
184 followed the protocol outlined by Lueders et al. (2004), and following extraction all samples were  
185 purified using the Qiaquick kit referenced above.

186 The V1V2 and V3 regions of the bacterial SSU rRNA gene were targeted for total  
187 community analysis using the universal bacterial primers 8F (5'-  
188 AGAGTTTGATCCTGGCTCAG- 3') and 529R (5'- CGCGGCTGCTGGCAC- 3'). The forward  
189 and reverse primers contained an Illumina Nextera XT overhang sequence that allowed for  
190 addition of multiplexing indices in a downstream PCR. Each 20  $\mu$ L PCR mixture contained  
191 approximately 1-5 ng of DNA, 0.001 mmol l<sup>-1</sup> of each primer, 2  $\mu$ g of BSA, and 10  $\mu$ L of KAPA  
192 HIFI HotStart ReadyMix (Kapa Biosystems Inc., Wilmington, MA). The PCR program was  
193 performed with the following cycling conditions: an initial denaturation at 95°C (3 min), followed  
194 by 25 cycles of denaturation at 98°C (20 s), annealing at 58°C (15 s), extension at 72°C (30 s),  
195 followed by a final extension at 72°C for 5 minutes. Following verification of the amplicon product  
196 in a 1.0% agarose gel, PCR products were cleaned and concentrated using the Qiaquick PCR  
197 Purification Kit, and quantified using a Qbit fluorometer (Invitrogen, Carlsbad, CA). The  
198 overhang-ligated amplicon products were further purified to remove free primers and primer  
199 dimers using the AMPure XP bead kit (Beckman Coulter Inc., CA, USA) following the Illumina  
200 instructions. Amplicons were subsequently barcoded using the Illumina Nextera XT index kit  
201 (Illumina, San Diego, CA) and purified a second time using the AMPure XP bead kit. Purified  
202 amplicon libraries were quantified using PicoGreen dsDNA reagent in 10 mmol l<sup>-1</sup> Tris buffer (pH  
203 8.0) (Thermo Fisher Scientific, Waltham, MA), pooled in equimolar amounts, spiked with 5%  
204 PhiX control spike-in, and sequenced via the paired end platform (2 x 300 bp) on an Illumina

205 MiSeq<sup>®</sup> with the v3 reagent kit. Amplicon sequences are available in the following GenBank SRA  
206 accession SRP127176.

207       Near full-length amplification of the SSU rRNA gene sequences was performed for DNA  
208 obtained from enrichment cultures and axenic isolates using primers 8F (see above) and 1492R  
209 (5'-TACGGYTACCTTGTTACGACTT-3') and the following PCR program: initial denaturation  
210 at 94°C (2 min), followed by 25 cycles of denaturation at 94°C (15 s), annealing at 51°C (15 s),  
211 extension at 72°C (100 s), and a final extension at 72°C for 5 minutes. Amplicons were cloned  
212 using the CloneJet PCR Cloning Kit (ThermoFisher Scientific, Waltham, MA) and 25 clones were  
213 sequenced at the Molecular Research Core Facility at Idaho State University in Pocatello, ID,  
214 USA. The near full-length clone sequences are deposited as GenBank accessions MG682464-  
215 MG382488. Along with enrichment sequencing, pure cultures were obtained from each  
216 enrichment through sequential streaking ( $\geq 3$  times) for isolation on solid BHI plates with  
217 333 mmol l<sup>-1</sup> urea and incubation at 30°C. Following isolations, one pure culture derived from the  
218 facultative and one from the anaerobic enrichment was targeted for full-length SSU rRNA gene  
219 sequencing using the primers and thermocycler conditions described above. The near full-length  
220 clone sequences can be found as GenBank accessions [MG674285-MG674286](#).

#### 221 *Pyrosequencing data and statistical analysis*

222 The SSU rRNA gene amplicon sequences for total community analysis were quality trimmed and  
223 refined using the Mothur pipeline following the Schloss laboratory's standard operating procedure  
224 (SOP) for MiSeq data sets (Kozich et al., 2013). In brief, the programs make.contigs and  
225 screen.seqs (maximum number of ambiguous bases = 0, maximum length = 550 bp), were used to  
226 identify high quality sequences. Duplicate sequences were removed to reduce computational times,  
227 and unique sequences were aligned to a reference alignment using the SILVA 16S rRNA gene

228 sequences from *Bacteria*. This alignment was customized to the area immediately surrounding the  
229 V1V2 and V3 regions. Poorly aligned as well as chimeric sequences were identified and removed  
230 from the data set. Next, taxonomic classifications were assigned using *classify.seqs*, and sequences  
231 identified as derived from either the domain *Archaea* or the chloroplast/mitochondria organelle  
232 were removed. To further reduce computation times, groups with sequences present at less than  
233 0.1% abundance were removed, thus focusing the analyses on abundant community members.  
234 These sequences were then binned into OTUs using the programs *dist.seqs* and *cluster*, and a  
235 representative sequence from each OTU was selected.

236         Representative sequences, near full-length clone libraries, and SSU rRNA gene sequences  
237 from isolated organisms were identified by comparison with known sequences in GenBank using  
238 BLASTn (<http://blast.ncbi.nlm.nih.gov/Blast.cgi>). Representative pyrosequencing reads were  
239 genus-level matches if they were  $\geq 80\%$  identical over  $\geq 80\%$  of the length of the read, while full-  
240 length clones were species-level matches if they were  $\geq 97\%$  identical over  $\geq 80\%$  of the length of  
241 the sequence.

#### 242 *Scanning Electron Microscopy*

243 Facultative and anaerobic enrichments were grown in CMM medium without NaCl for  
244 microscopy. The cells were prepared for imaging by immobilization on a glass slide and then  
245 mounted and coated with iridium for imaging (1 kV) with a Zeiss Supra 55 Field Emission  
246 Scanning Electron Microscope (FE-SEM) at the Image and Chemical Analysis Laboratory (ICAL)  
247 at Montana State University.

248

## 249 **Results**

### 250 *Habitat and Enrichment*

251 Enrichment cultures for ureolytic microorganisms were prepared using sediment slurry samples  
252 collected at three shore-line locations at Soap Lake (site SL2), Alkali Lake (Site SL3), and  
253 Lenore Lake (Site SL4), a series of saline and alkaline lakes located in central Washington  
254 (Figure S1A). The pH values ranged between 9.05 and 9.85, with all water temperatures at 2°C.  
255 CMM containing urea was inoculated in triplicate with sediment slurries and incubated in the  
256 dark at 37°C without shaking. Abiotic controls without inoculum were also tracked alongside the  
257 enrichment cultures. Significant ureolysis (defined as  $\geq 50\%$  decrease in the urea concentration)  
258 was detected after 30 days in the facultative and anaerobic enrichments established from site SL2  
259 sediment slurries (Figure S1B), and positive cultures were transferred into fresh medium. Abiotic  
260 controls showed no decrease in urea concentrations after 30 days. In an initial set of experiments,  
261 ureolysis efficacy and mineral precipitation were assessed in both the anaerobic and facultative  
262 SL2 enrichments by tracking urea,  $\text{Ca}^{2+}$ , and alkalinity levels over a ten-hour period. Decreases  
263 in urea (Figure 1A) and an increase in both medium pH (Figure 1B) and alkalinity (Figure 1D)  
264 indicated that ureolysis occurred in both enrichment cultures and that carbonate was produced. A  
265 roughly 33% reduction in the starting concentration of urea ( $333 \text{ mmol l}^{-1}$ ) was observed over 10  
266 hours. This, combined with the observation of increased pH and alkalinity, verified that  
267 significant ureolysis occurred, resulting in the alkaline microenvironment necessary for  
268 carbonate mineral precipitation. Dissolved Ca concentrations were also tracked and used as a  
269 proxy for  $\text{CaCO}_3$  precipitation (Figure 1C). Initial Ca concentrations were approximately  $0.033$   
270  $\text{mol l}^{-1} \text{ CaCl}_2 \cdot 2\text{H}_2\text{O}$ . Ca concentrations decreased below the detection limit by the end of the 10-  
271 hour experiment (Figure 1C) in both enrichments, indicating that less than  $1.25 \cdot 10^{-4} \text{ mol l}^{-1}$  of the  
272 initial Ca concentration remained. Finally, mineral precipitates were characterized using Raman  
273 Spectromicroscopy, which identified calcite ( $\text{CaCO}_3$ ) as main mineral phase in all samples

274 (Figure S2). The abiotic control samples showed no visible precipitates, and thus were not  
275 analyzed using Raman Spectromicroscopy.

#### 276 *Optimal Growth Conditions and S. pasteurii Tolerance Comparison*

277 Facultative enrichments from site SL2 grew optimally at 30°C but were capable of growth  
278 between 20°C and 40°C (Figure 2A). Similarly, the pH tolerance for this enrichment culture  
279 appeared to be broad, displaying growth across the entire pH 6-11 range at 30°C (Figure 2A).  
280 The SL2 facultative enrichment also grew across a wide range of salinities (0-100 g l<sup>-1</sup> NaCl) at  
281 30°C and a pH of 9, with optimal growth observed at 50 g l<sup>-1</sup> (Figure 2D).

282 In contrast to the wide growth spectrum of the facultative enrichment, SL2 ureolytic  
283 enrichments cultivated under anaerobic conditions displayed a more restricted growth range.  
284 Limited growth was observed for the anaerobic SL2 enrichment after 24 hours across the entire  
285 tested temperature range (Figure 2B), though a slight preference for 30°C was noted. The optimal  
286 and pH and salinity ranges were pH 8 at 30°C and 25 g l<sup>-1</sup> NaCl at 30°C and pH 8, respectively  
287 (Figure 2B and 2E).

288 Additional experiments examined optimal conditions for *S. pasteurii* strain ATCC 11859  
289 to determine its requirements and tolerance for growth under aerobic conditions. An initial set of  
290 experiments revealed that strain ATCC 11859 was incapable of growth in CMM medium that did  
291 not contain urea. Knowing that the inclusion of urea would initiate ureolysis, and significantly  
292 alter the pH of the medium, an alternative cultivation medium, BHI broth, was employed instead.  
293 Figure 2C shows that strain 11859 grew best at 30°C, with a growth range of 22 to 40°C. *S.*  
294 *pasteurii* strain 11859 also appeared to be adapted to alkaline environments, displaying  
295 significant growth at pH values ranging from 6 to 11 at 30°C (Figure 2C). Finally, though  
296 optimum growth was achieved in the absence of additional NaCl, *S. pasteurii* strain 11859

297 appeared to be halotolerant, with growth observed in cultures with NaCl concentrations up to 75  
298 g l<sup>-1</sup> at 30°C and pH 8 (Figure 2F).

### 299 *Community Analysis*

300 Initial bacterial community characterizations were performed for site SL2 (Figure 3) and at  
301 sampling locations SL3 and SL4 (Supporting Information Figure S3). Operational taxonomic  
302 unit (OTU) richness (at 97% sequence identity) indicated a large proportion (67%) of the  
303 baseline SL2 community were unclassified genera with predominant identified populations most  
304 closely related to the well-known alkaliphilic bacterium *Microcella* (9% abundance), the  
305 bacterium *Pullulanibacillus* (6% abundance), and the cyanobacterium *Synechococcus* (6%  
306 abundance) (Figure 3). Shifts in genus-level relative abundance were apparent in the Illumina  
307 SSU rRNA-based analysis following ureolytic enrichments, where *Bacillus* was the only genus  
308 with an abundance of ≥1% in the facultative enrichment, while the obligate anaerobic  
309 community was comprised of a mixture of *Bacillus* (39% abundance) and the obligate anaerobic  
310 genus *Clostridium* (60% abundance) (Figure 3). This is in contrast to the baseline SL2  
311 populations, where the genus *Bacillus* was present at approximately 3% abundance and  
312 *Clostridium* populations were below 1% relative abundance.

313         Recent work taxonomically reclassified several *Bacillus* genera as belonging to the genus  
314 *Sporosarcina* based on distinct phylogenetic and cellular properties (Yoon et al., 2001). To  
315 determine whether short Illumina sequence reads identified as *Bacillus* across the V1-V3 rRNA  
316 gene region were potentially *Sporosarcina* members, full-length SSU rRNA gene clones were  
317 used to obtain species-level identification of enriched populations. All full-length clones from  
318 the facultative ureolytic enrichment were a close gene sequence match (99% sequence similarity)  
319 to *S. pasteurii* strain NCCB 48021 (Figure 3), while anaerobic SL2 enrichment clones were a

320 mixture of cultivated relatives of *Clostridium* sp. MT1 and *S. pasteurii* strain NCCB 48021  
321 (Figure 3). For both enrichment cultures, the clone sequencing indicated that other potential  
322 organisms were present at abundance levels likely no greater than 4%. Along with these clone  
323 libraries, one isolate from each enrichment was analyzed via full-length rRNA gene sequencing.  
324 Results supported the clone library results, where both the facultative and anaerobic ureolytic  
325 isolates were a close gene sequence match (99% sequence similarity) to *S. pasteurii* strain NCCB  
326 48021. SEM images of the enrichment cultures also support the genus-level identification, where  
327 numerous rod-shaped morphologies were detected under both culture conditions (Figure 4),  
328 which correlates to known morphologies for both *S. pasteurii* and *Clostridium*.

### 329 *Rates of Precipitation*

330 Urea concentrations and direct cell counts were tracked in SL2 enrichment cultures and the  
331 MICP type strain *S. pasteurii* ATCC 11859 to determine ureolytic activity on a per cell basis.  
332 Ureolytic activities were calculated by normalizing the moles of urea hydrolyzed per hour by the  
333 cell density. Interestingly, no lag phase in growth was detected in either of the SL2 enrichments,  
334 while growth of the MICP model strain *S. pasteurii* ATCC 11859 appeared to be delayed for  
335 approximately 2 hours following inoculation (Table 1). The obligate anaerobic enrichment  
336 communities from site SL2 displayed the highest cell-specific urea hydrolysis rates, peaking at  
337  $3.05 \cdot 10^{-10} \pm 2.40 \cdot 10^{-11}$  moles of urea hydrolyzed  $\cdot \text{cell}^{-1} \cdot \text{hr}^{-1}$  (Table 1). A two-tail Student's *t*-test  
338 assuming equal variances determined this activity level was statistically significant ( $P < 0.01$ )  
339 when compared to both the facultative SL2 enrichment as well as *S. pasteurii* ATCC 11859.  
340 Urea hydrolysis rates for the model MICP organism and the facultative SL2 enrichment cultures  
341 were comparable and averaged between  $1.05 \cdot 10^{-10}$  to  $1.95 \cdot 10^{-10}$  moles of urea hydrolyzed  $\cdot \text{cell}^{-1} \cdot \text{hr}^{-1}$ .  
342

343

344 **Discussion**

345 One challenge identified in scaling up MICP-based sealing applications to the field lies in the  
346 availability of organisms adapted to the geochemical and geological conditions present in the  
347 deeper subsurface (Phillips et al. 2013, 2016). To date, biomineralization sealing studies have  
348 largely focused on the use of *S. pasteurii* strains, though its long-term persistence under  
349 anaerobic conditions is doubtful (Martin et al., 2012), and its ability to conduct ureolysis in deep  
350 saline aquifers is unknown (Mortensen et al., 2011). The work presented here enriched and  
351 identified bacterial populations, which increase the versatility and potential applicability of the  
352 biomineralization sealing technology beyond the current range. Using haloalkaliphilic media,  
353 either devoid of or containing minimal oxygen, we enriched for and identified ureolytically  
354 active bacterial populations potentially more suitable for deep subsurface environments.

355 An emerging need in commercializing biomineralization-based technologies is that  
356 suitable organisms be able to reliably precipitate CaCO<sub>3</sub> in anaerobic subsurface habitats. This  
357 study shows that enrichment of efficient facultative and anaerobic ureolytic bacteria from an  
358 alkaline soda lake environment may provide good alternatives to the obligate aerobic bacterium  
359 *S. pasteurii* ATCC 11859 or other reference strains. To date, anaerobic growth has only been  
360 observed using alternative carbonate mineral-forming metabolisms such as denitrification (van  
361 Paassen et al., 2010; Martin et al., 2012; Hamdam et. al., 2016), sulfate reduction (Wright and  
362 Wacey, 2005), and iron reduction (Zeng and Tice, 2014). Each one of these alternate  
363 metabolisms generally results in slower growth rates than aerobic respiration, and since mineral  
364 precipitation-inducing reactions for these metabolisms are growth-dependent, precipitation rates  
365 are generally slower. Urea hydrolysis can be growth-independent, thus the ability of an organism  
366 to promote high rates of ureolysis while growing in the absence of oxygen might be central to

367 reliably implementing ureolysis-induced mineral precipitation strategies in the deep subsurface.  
368 Along with the ability to promote growth and ureolysis anaerobically, work here also shows that  
369 it can occur across NaCl concentrations ranging from 0-100 g l<sup>-1</sup>, and at pH values as high as 11  
370 (Figure 2A, 2B, 2D, 2E). This indicates that the anoxic, high-pH, and high salinity conditions  
371 potentially present in deep saline aquifers could be suitable for the growth of ureolytic  
372 haloalkaliphilic organisms. Interestingly, by examining optimal growth conditions of the MICP  
373 model strain we also better defined the potential application range of *S. pasteurii* ATCC 11859  
374 (Figure 2C, 2F), observing that it can reliably grow across salinities up to 75 g l<sup>-1</sup>. This range far  
375 exceeds previously tested values which mimicked oceanic seawater (26.7 g l<sup>-1</sup>) conditions  
376 (Mortensen et al., 2011) and supports the potential applicability of *S. pasteurii* to be used in deep  
377 (aerobic) saline aquifers which are a target environment for carbon capture and storage, as well  
378 as enhanced oil recovery.

379       Enrichment of haloalkaliphilic bacteria capable of hydrolyzing urea was not unexpected  
380 given the widespread detection of the *ureC* functional subunit in sediment and groundwater  
381 environments (Fujita et al., 2008), as well as the estimate that between 17 and 30% of cultivated  
382 species from soil habitats are capable of urea hydrolysis (Lloyd and Sheaffe, 1973). Previous  
383 work isolating ureolytic bacteria from soil habitats also observed that >50% of cultivated isolates  
384 were members of the *Sporosarcina* genus (Burbank et al., 2012), explaining the likelihood of  
385 enriching *S. pasteurii*-like strains. The inclusion of 333 mmol l<sup>-1</sup> urea in the enrichment medium  
386 was also likely to result in conditions inhibitory to many species, due to the accumulation of  
387 ammonia and high pH values, thus potentially selecting for bacteria capable of constitutive  
388 urease expression and tolerance to high pH values and ammonium concentrations, of which few  
389 have been identified (Burbank et al., 2012).

390 Previous work demonstrated that *S. pasteurii* cannot synthesize urease under anaerobic  
391 conditions (Martin et al., 2012). In studies reported here, we enrich for a strain of *S. pasteurii*  
392 most closely related to strain NCCB 48021 under both facultative and obligate anaerobic  
393 conditions, therefore potentially overcoming known challenges with the deep subsurface  
394 application of the MICP model strain *S. pasteurii* ATCC 11859.

395 Along with *S. pasteurii*, a *Clostridium* species was also enriched in the anaerobic SL2  
396 culture. Isolation of individual bacterial organisms was not a priority in the current work, as we  
397 envision utilizing mixed communities of biomineralizing microorganisms suited to specific  
398 down-hole environments for engineered applications. Using high-throughput SSU rRNA gene  
399 amplicon sequencing and clone libraries, obligate anaerobic ureolytic enrichment communities  
400 from site SL2 were observed to contain a mixture of a *S. pasteurii* strain most closely related to  
401 strain NCCB 48021 and a *Clostridium* sp. most closely related to strain MT1 (Figure 3). The  
402 enrichment of an obligate anaerobe like this *Clostridium* strain indicates that conditions in the  
403 enrichment culture were indeed anaerobic. While it is unclear whether enriched *Clostridium*  
404 populations were actively contributing to urea hydrolysis, several *Clostridium* species are known  
405 to be urease positive (Mobley and Hausinger, 1989), carrying their urease structural genes on a  
406 plasmid, and only activating urease gene expression under nitrogen deplete conditions (Dupuy et  
407 al., 1997). Further testing is needed to determine the potential functional role of *Clostridium* spp.  
408 in the anaerobic enrichment cultures.

409 The economic feasibility of MICP-based fracture sealing depends on high ureolytic  
410 activity and efficient CaCO<sub>3</sub> precipitation. To develop a bioinventory for field deployment,  
411 microorganisms must be able to remain ureolytically active, and ideally grow, under *in situ*  
412 conditions. These properties will help ensure subsurface leakage pathways are sealed in a

413 reasonable time frame. Results presented here indicate that the rate of urea removal on a per-cell  
414 basis in the SL2 haloalkaliphilic anaerobic communities was statistically greater ( $P < 0.01$ ) than  
415 the *S. pasteurii* ATCC 11859 strain (Table 1), suggesting increased urea hydrolysis rates in the  
416 anaerobic SL2 enrichment may well be due to higher urease enzyme activity on a per cell basis.  
417 Interestingly, for both SL2 enrichment cultures, ureolysis started within the first two hours  
418 following inoculation, and once initiated, took roughly 8 hours for >95% of 333 mmol l<sup>-1</sup> urea to  
419 be hydrolyzed (data not shown). Experiments here did not attempt to optimize either urea or Ca<sup>2+</sup>  
420 concentrations, both of which are parameters known to influence the CaCO<sub>3</sub> precipitation levels  
421 (Krajewska 2018), suggesting further optimization of the MICP process is possible.

422         In summary, several challenges exist in continuing to move toward broader field-scale  
423 implementations of MICP-based technologies. These challenges include costs associated with  
424 the injection and growth of MICP organisms on a large scale, variability of conditions commonly  
425 experienced in the subsurface, as well as ensuring proper biosafety and environmental  
426 protections (Krajewska 2018; Ivanov et al., 2019). Knowing that saline aquifers are a primary  
427 target for CO<sub>2</sub> sequestration and that subsurface fractures may serve as CO<sub>2</sub> leakage routes,  
428 microorganisms used in MICP treatment need to be tailored to high-salinity and high-  
429 temperature environments that are likely either microaerobic or completely anoxic. These saline  
430 aquifers are also known to vary widely with respect to pH conditions. MICP has been used at  
431 least twice to seal fractures at relevant depths (310-340 m) using the model organism *S. pasteurii*  
432 (Phillips et al., 2016, 2018) in an environment that was moderately acidic (pH 5.5), brackish (24  
433 g l<sup>-1</sup> NaCl), and likely microaerophilic (-16 mV ORP). We present evidence here that highly  
434 ureolytically active microbial communities with specific adaptation to high-pH and high-salinity  
435 environments can be successfully isolated under anaerobic conditions, and that this consortium

436 of bacteria can add to the possible suite of organisms available for MICP implementation. We  
437 also show that extreme environments like those at Soap Lake can harbor microbial community  
438 members which produce large quantities of active urease, making them potentially useful for  
439 engineered biomineralization technologies. Further research and development efforts are needed  
440 to develop a collection of ureolytically active organisms suitable for the range of other conditions  
441 likely encountered at subsurface application sites, most notably increased temperature and  
442 pressure.

443

#### 444 **Acknowledgements**

445 This research was supported by the U.S. Department of Energy (DOE) Small Business  
446 Technology Transfer (STTR) Program contract no. DE-FG02-13ER86571 (“Using  
447 Biomineralization Sealing for Leakage Mitigation in Shale during CO<sub>2</sub> Sequestration”). Arda  
448 Akyel was supported by the Thermal Biology Institute through funding from the MSU Office of  
449 the Vice President for Research and Economic Development for Ph.D. graduate enhancement.  
450 Our thanks are extended to Sara Altenburg for her help with SEM imaging, Dr. Erika J.  
451 Espinosa-Ortiz for confocal Raman Spectromicroscopy analysis, and Dr. Logan Schultz for  
452 sample collection.

453

#### 454 **Conflicts of Interest**

455 The authors have no conflicts of interest to declare.

456

#### 457 **References**

458 Achal V., Pan X., Fu Q., and Zhang D. (2012) Biomineralization based remediation of As(III)  
459 contaminated soil by *Sporosarcina ginsengisoli*. *J Hazard Mater* **201**, 178–184.

460  
461 Bang S., Galinat J., and Ramakrishnan V. (2001) Calcite precipitation induced by polyurethane-  
462 immobilized *Bacillus pasteurii*. *Enzyme Microb Technol* **28**, 404–409.  
463  
464 Bassett R.L. and Bentley M.E. (1983) Deep brine aquifers in the palo duro basin: regional flow  
465 and geochemical constraints. *Bureau of Economic Geology* **130**, 1-59.  
466  
467 Burbank M.B., Weaver T.J., Williams B.C., and Crawford R.L. (2012) Urease activity of ureolytic  
468 bacteria isolated from six soils in which calcite was precipitated by indigenous bacteria.  
469 *Geomicrobiol J* **29**, 389-395.  
470  
471 DeJong J.T., Fritzsche M.B., and Nüsslein K. (2006) Microbially induced cementation to control  
472 sand response to undrained shear. *J Geotech Geoenviron Eng* **132**, 1381–1392.  
473  
474 Dupuy B., Daube G., Popoff M.R., and Cole S.T. (1997) *Clostridium perfringens* urease genes are  
475 plasmid borne. *Infect Immun* **65(6)**, 2313-2320.  
476  
477 Ferris F., Stehmeier L., Kantzas A., and Mourits F. (1996) Bacteriogenic mineral plugging. *J Can*  
478 *Petrol Technol* **35**, 56–61.  
479  
480 Fidaleo M. and Lavecchia R. (2003) Kinetic study of enzymatic urea hydrolysis in the pH range  
481 4–9. *Chem Biochem Eng Q* **17**, 311–318.  
482  
483 Fujita Y., Taylor J., Wendt L., Reed D., and Smith R. (2010) Evaluating the potential of native  
484 ureolytic microbes to remediate a (90)Sr contaminated environment. *Environ Sci Technol* **44**,  
485 7652–7658.  
486  
487 Hamdam N., Kavazanjian Jr. E., Rittmann B.E., and Karatas I. (2016) Carbonate mineral  
488 precipitation for soil improvement through microbial denitrification. *Geomicrobiol J* 1-8.  
489  
490 Ivanov, V., Stabnikov, V., Stabnikova, O., and Kawasaki, S. (2019) Environmental safety and  
491 biosafety in construction biotechnology. *World J Microb Biot* **35**:26.  
492  
493 Jonkers H.M., Thijssen A., Muyzer G., Copuroglu O., and Schlangen E. (2010) Application of  
494 bacteria as self-healing agent for the development of sustainable concrete. *Ecol Eng* **36**, 230–235.  
495  
496 Jung D., Biggs H., Erikson J., and Ledyard P.U. (1975) New colorimetric reaction for end-point,  
497 continuous-flow, and kinetic measurement of urea. *Clin Chem* **21(8)**, 1136-1140.  
498  
499 Kanagasabapathy A.S. and Kumari, S. (2000) *Guidelines on Standard Operating Procedures for*  
500 *Clinical Chemistry*. Regional Office for South-East Asia, New Delhi: World Health Organization,  
501 p. 59-62.  
502  
503 Kozich J.J., Westcott S.L., Baxter N.T., Highlander S.K., and Schloss P.D. (2013) Development  
504 of a dual-index sequencing strategy and curation pipeline for analyzing amplicon sequence data  
505 on the miseq illumina sequencing platform. *Appl Environ Microb* **79(17)**, 5112-5120.

506  
507 Krajewska, B. (2018) Urease-aided calcium carbonate mineralization for engineering applications:  
508 a review. *J Adv Res* **13**, 59-67.  
509  
510 Lauchnor, E., Schultz, L., Bugni, S., Mitchell, A., Cunningham, A., and Gerlach, R. (2013)  
511 Bacterially induced calcium carbonate precipitation and strontium coprecipitation in a porous  
512 media flow system. *Environ Sci Technol* **47**, 1557-1564.  
513  
514 Lueders, T., Manefield, M., and Friedrich, M.W. (2004) Enhanced sensitivity of DNA- and rRNA-  
515 based stable isotope probing by fractionation and quantitative analysis of isopycnic centrifugation  
516 gradients. *Environ Microbiol* **6(1)**, 73-78.  
517  
518 Lloyd A.B., and Sheaffe M.J. (1973) Urease activity in soils. *Plant Soils* **39**, 71–80.  
519  
520 Martin D., Dodds K., Ngwenya B., Butler I., and Elphick S. (2012) Inhibition of *Sporosarcina*  
521 *pasteurii* under anoxic conditions: implications for subsurface carbonate precipitation and  
522 remediation via ureolysis. *Environ Sci Technol* **46**, 8351–8355.  
523  
524 Martin D., Dodds K., Butler I.B., and Ngwenya B.T. (2013) Carbonate precipitation under pressure  
525 for bioengineering in the anaerobic subsurface via denitrification. *Environ Sci Technol* **47**, 8292-  
526 8699.  
527  
528 Mitchell A.C., Dideriksen K., Spangler L., Cunningham A., and Gerlach R. (2010) Microbially  
529 enhanced carbon capture and storage by mineral-trapping and solubility-trapping. *Environ Sci*  
530 *Technol* **44**, 5270–5276.  
531  
532 Mobley H.L., and Hausinger R.P. (1989) Microbial ureases: significance, regulation, and  
533 molecular characterization. *Microbiol Rev* **53**, 85–108.  
534  
535 Mortensen B., Haber M., DeJong J., Caslake L., and Nelson D. (2011) Effects of environmental  
536 factors on microbial induced calcium carbonate precipitation. *J Appl Microbiol* **111**, 338–349.  
537  
538 Phillips, A.J. (2013a) Biofilm-Induced Calcium Carbonate Precipitation: Application in the  
539 Subsurface. Ph.D. Dissertation, Montana State University, Bozeman, MT.  
540  
541 Phillips A.J., Lauchnor E., Eldring, J., Esposito M., Mitchell A.C., Gerlach R., Cunningham A.B.,  
542 and Spangler L.H. (2013b) Potential CO<sub>2</sub> leakage reduction through biofilm-induced calcium  
543 carbonate precipitation. *Environ Sci Technol* **47**, 142–149.  
544  
545 Phillips A.J., Cunningham A.B., Gerlach R., Hiebert R., Hwang C., Lomans B.P., Westrich J.,  
546 Mantilla C., Kirksey J., Esposito R., and Spangler L.H. (2016) Fracture sealing with microbially-  
547 induced calcium carbonate precipitation: A Field Study. *Environ Sci Technol* **50**, 4111–4117.  
548  
549 Phillips, A. J., Troyer, E., Hiebert, R., Kirkland, C., Gerlach, R., Cunningham, A. B., Spangler, L.,  
550 Kirksey, J., Rowe, W., and Esposito, R. (2018). Enhancing wellbore cement integrity with

551 microbially induced calcite precipitation (MICP): A field scale demonstration. *J Petroleum Sci*  
552 *Eng* **171**, 1141-1148.

553

554 Rusu C., Cheng X., and Li M. (2011) Biological clogging in Tangshan sand columns under salt  
555 water intrusion by *Sporosarcina pasteurii*. *Adv Mater Res* **250**, 2040–2046.

556

557 Stocks-Fischer S., Galinat J., and Bang S. (1999) Microbiological precipitation of CaCO<sub>3</sub>. *Soil*  
558 *Biol Biochem* **31**, 1563–1571.

559

560 Tobler D.J., Cuthbert M.O., Greswell R.B., Riley M.S., Renshaw J.C., Handley-Sidhu S., and  
561 Phoenix V.R. (2011) Comparison of rates of ureolysis between *Sporosarcina pasteurii* and an  
562 indigenous groundwater community under conditions required to precipitate large volumes of  
563 calcite. *Geochim Cosmochim AC* **75**, 3290–3301.

564

565 van Paassen L.A., Daza C.M., Staal M., Sorokin D.Y., van der Zon W., and Loosdrecht M.C.M.  
566 (2010) Potential soil reinforcement by biological denitrification. *Ecol Eng* **36**, 168–175.

567

568 Whiffin V.S., van Paassen L., and Harkes M. (2007) Microbial carbonate precipitation as a soil  
569 improvement technique. *Geomicrobiol J* **24**, 417–423.

570

571 Wright D.T. and Wacey D. (2005) Precipitation of dolomite using sulphate-reducing bacteria from  
572 the Coorong Region, South Australia: significance and implications. *Sedimentology* **52(5)**, 987-  
1008.

573

574 Yoon, J.H, Lee, K.C., Weiss, N., Kho, Y.H., Kang, K.H., and Park, Y.H. (2001) *Sporosarcina*  
575 *aquimarina* sp. nov., a bacterium isolated from seawater in Korea, and transfer of *Bacillus*  
576 *globisporus* (Larkin and Stokes 1967), *Bacillus psychrophilus* (Nakamura 1984) and *Bacillus*  
577 *pasteurii* (Chester 1898) to the genus *Sporosarcina* as *Sporosarcina globispora* comb. nov.,  
578 *Sporosarcina psychrophila* comb. nov. and *Sporosarcina pasteurii* comb. nov., and emended  
description of the genus *Sporosarcina*. *Int J Syst Evol Micr* **51**, 1079-1086.

579

580 Zeng Z. and Tice M.M. (2014) Promotion and nucleation of carbonate precipitation during  
microbial iron reduction. *Geobiology* **12(4)**, 362-371.

581

582

583

584

585

586

587

588 **Tables****Table 1.** Summary of urea hydrolysis rates

Enrichment/Culture	Rate (moles urea hydrolyzed cell <sup>-1</sup> h <sup>-1</sup> )	Lag time
SL2 Facultative	1.05·10 <sup>-10</sup> +/- 1.70·10 <sup>-11</sup>	<2 hr
SL2 Anaerobic	3.05·10 <sup>-10</sup> +/- 2.40·10 <sup>-11</sup>	<2 hr
<i>S. pasteurii</i>	1.94·10 <sup>-10</sup> +/- 8.20·10 <sup>-12</sup>	2 hr

589  
590  
591  
592  
593  
594  
595  
596  
597  
598  
599  
600  
601  
602  
603  
604  
605  
606  
607  
608  
609  
610  
611  
612  
613  
614  
615  
616  
617  
618  
619  
620  
621  
622  
623

624 **Figure Legends**

625 **Figure 1.** Liquid analysis of SL2 enrichment cultures (CMM medium, pH 6, 50 g l<sup>-1</sup> NaCl, 333  
626 mmol l<sup>-1</sup> Urea) with 0.033 mol l<sup>-1</sup> CaCl<sub>2</sub>\*2H<sub>2</sub>O. (A) Urea, (B) pH, (C) dissolved calcium levels,  
627 and (D) alkalinity were tracked every two hours in facultative (white symbols) and anaerobic  
628 (black symbols) enrichments from Soap Lake location SL2. An uninoculated abiotic control  
629 (diamonds) was also included to assess the potential for abiotic ureolysis and precipitation.

630

631 **Figure 2.** OD<sub>600nm</sub> measured after 24 hours for facultative (A, D) and anaerobic (B, E) SL2  
632 enrichments, as well as *S. pasteurii* strain ATCC 11859 (C, F). Shown are the maximal optical  
633 densities for salinity (▲), temperature (■), and pH (●) determined as specified in the materials and  
634 methods section.

635

636 **Figure 3.** Taxonomic diversity and richness at sampling site SL2 at the time of sample collection  
637 (baseline community) and following enrichment under facultative and anaerobic conditions. The  
638 left panel shows species-level diversity and richness in full-length 16S rRNA clone libraries from  
639 the enrichment cultures, while the right panel depicts genus-level 16S rRNA genes identified from  
640 Illumina-sequenced amplicon libraries. Only genera with a relative abundance ≥1% are shown.

641

642 **Figure 4.** Microbial communities enriched from an aqueous sample collected on the southeast  
643 shore of Soap Lake (site SL2). Field-Emission Scanning Electron Microscopy (FE-SEM) images  
644 of SL2 samples enriched under (A) facultative and (B) anaerobic conditions indicate the presence  
645 of numerous rod-shaped morphologies under both enrichment conditions.

646

647

648

649 **Figure Legends for Supporting Information**

650 **Figure S1.** Soap Lake location and the sites selected for sample enrichment. The map (A)  
651 illustrates Soap Lake and surrounding areas with an arrow depicting the approximate location of  
652 sites SL2, SL3, and SL4 while images and inset (B) highlight the precise sampling location of site  
653 SL2.

654

655 **Figure S2.** Raman spectra shown for mineral precipitates formed in facultative (A) and anaerobic  
656 (B) SL2 enrichments. A reference spectrum for calcite is displayed in orange while the acquired  
657 spectra are displayed in black.

658

659 **Figure S3.** Relative abundance of major genus-level clades at two high pH and high salinity  
660 locations in the Soap Lake (WA) drainage. The relative abundance of a genus is proportional to  
661 the area of the circle, as depicted by the scale bar on the bottom. Only genera with a relative  
662 abundance  $\geq 1\%$  are shown.

663

664 **Table S1.** Aqueous Geochemistry

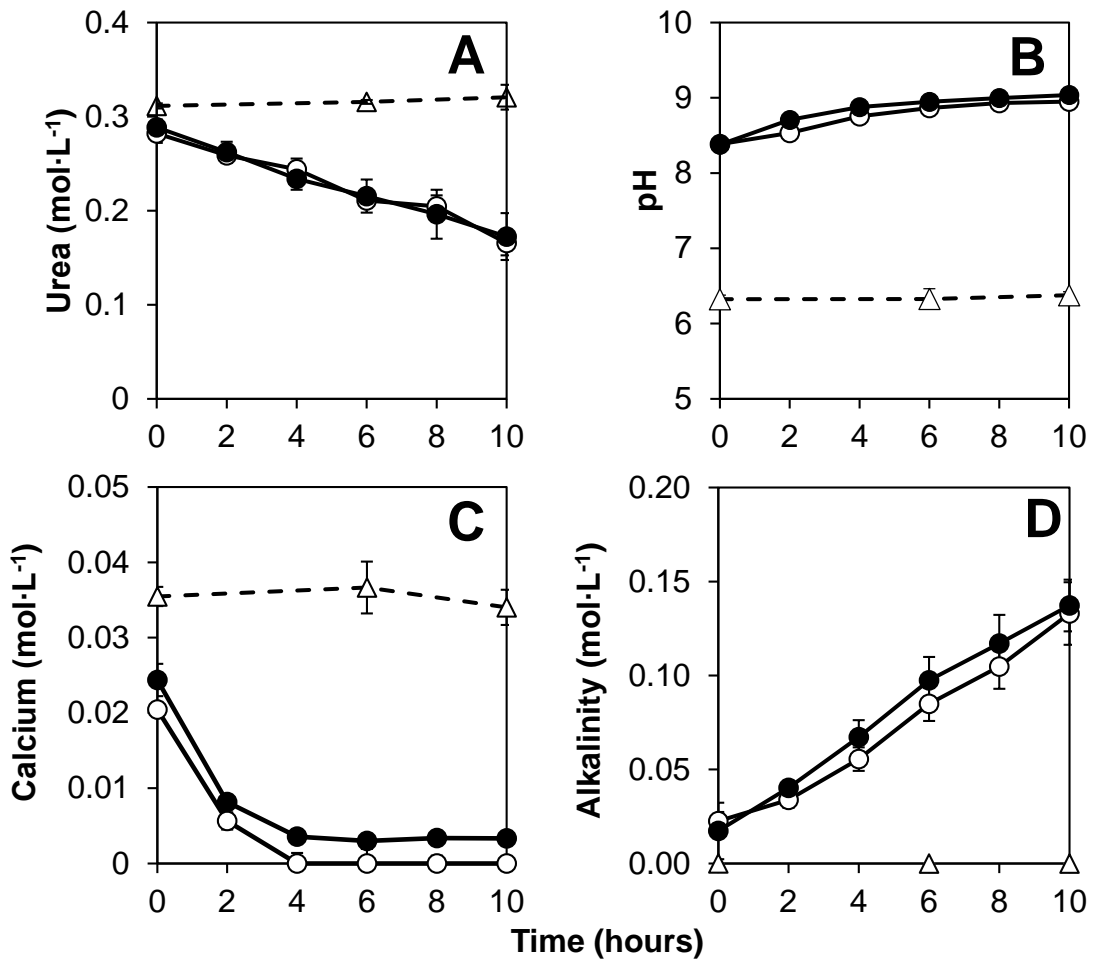


**Figure 1.** Liquid analysis of SL2 enrichment cultures (CMM medium, pH 6, 50 g·L<sup>-1</sup> NaCl, 333 mmol·L<sup>-1</sup> Urea) with 0.033 mol·L<sup>-1</sup> CaCl<sub>2</sub>·2H<sub>2</sub>O. (A) Urea, (B) pH, (C) dissolved calcium levels, and (D) alkalinity were tracked every two hours in facultative (white symbols) and anaerobic (black symbols) enrichments from Soap Lake location SL2. An uninoculated abiotic control (diamonds) was also included to assess the potential for abiotic ureolysis and precipitation.

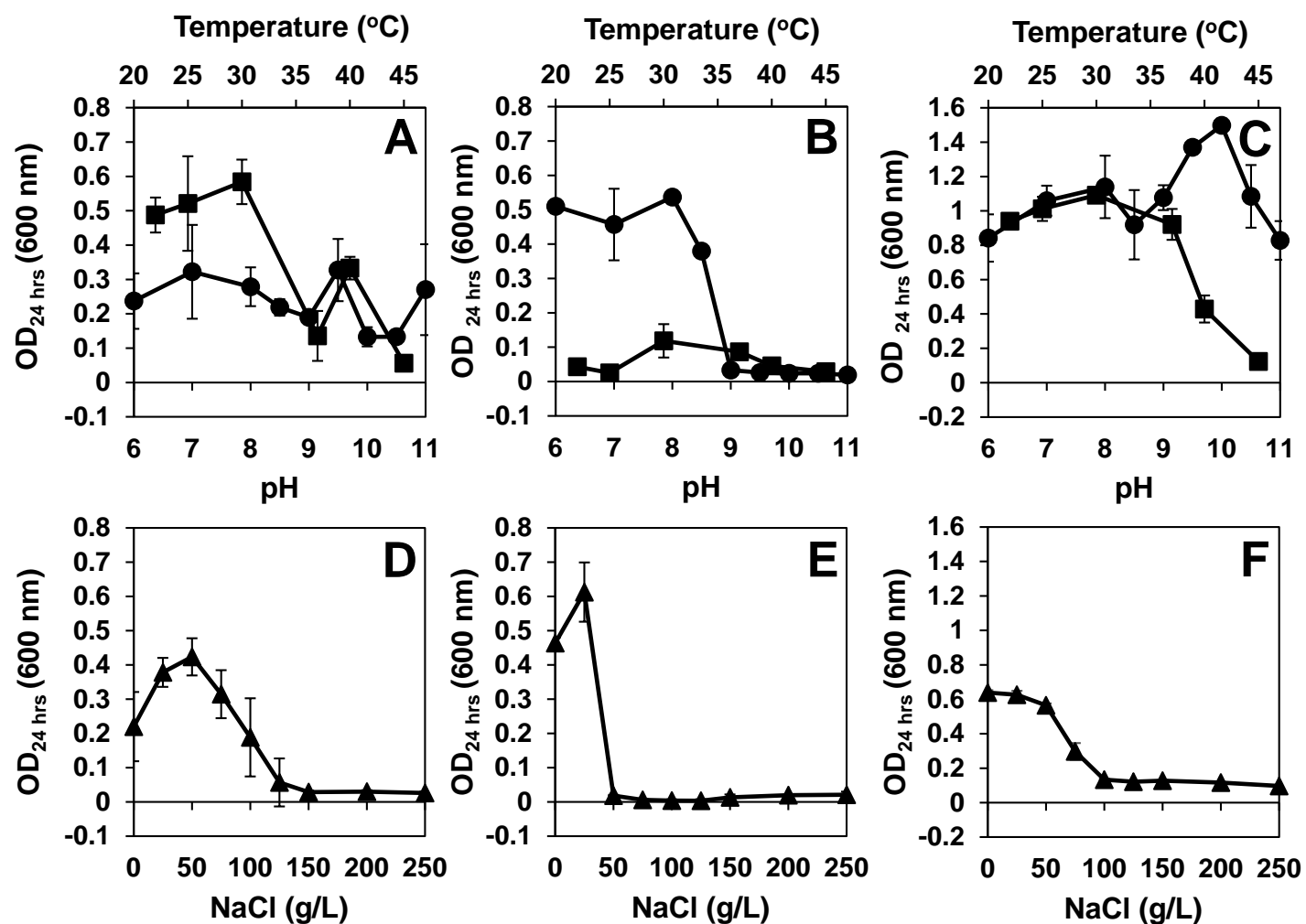


**Figure 2.** OD<sub>600 nm</sub> measured after 24 hours for facultative (A, D) and anaerobic (B, E) SL2 enrichments, as well as *S. pasteurii* strain ATCC 11859 (C, F). Shown are the maximal optical densities for temperature (■), pH (●) and salinity (▲) determined as specified in the materials and methods section.

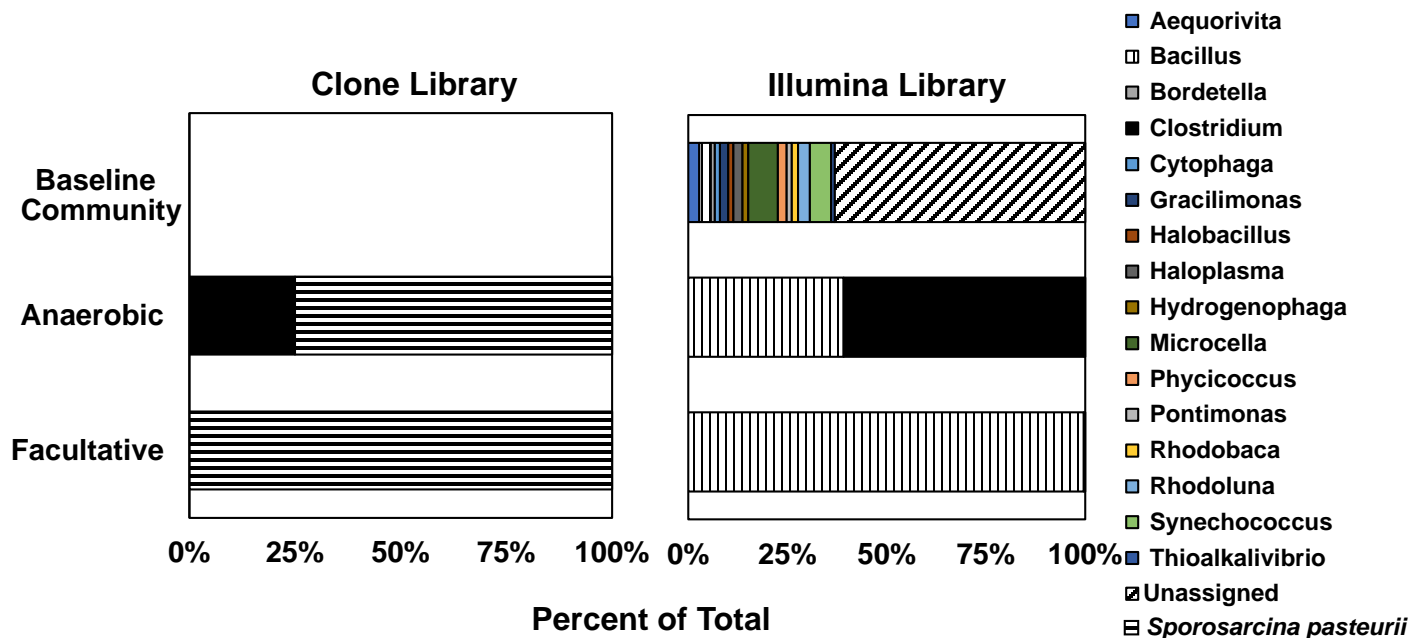


**Figure 3.** Taxonomic diversity and richness at sampling site SL2 at the time of sample collection (baseline community) and following enrichment under facultative and anaerobic conditions. The left panel shows species-level diversity and richness in full-length 16S rRNA clone libraries from the enrichment cultures, while the right panel depicts genus-level 16S rRNA genes identified from Illumina-sequenced amplicon libraries. Only genera with a relative abundance  $\geq 1\%$  are shown.

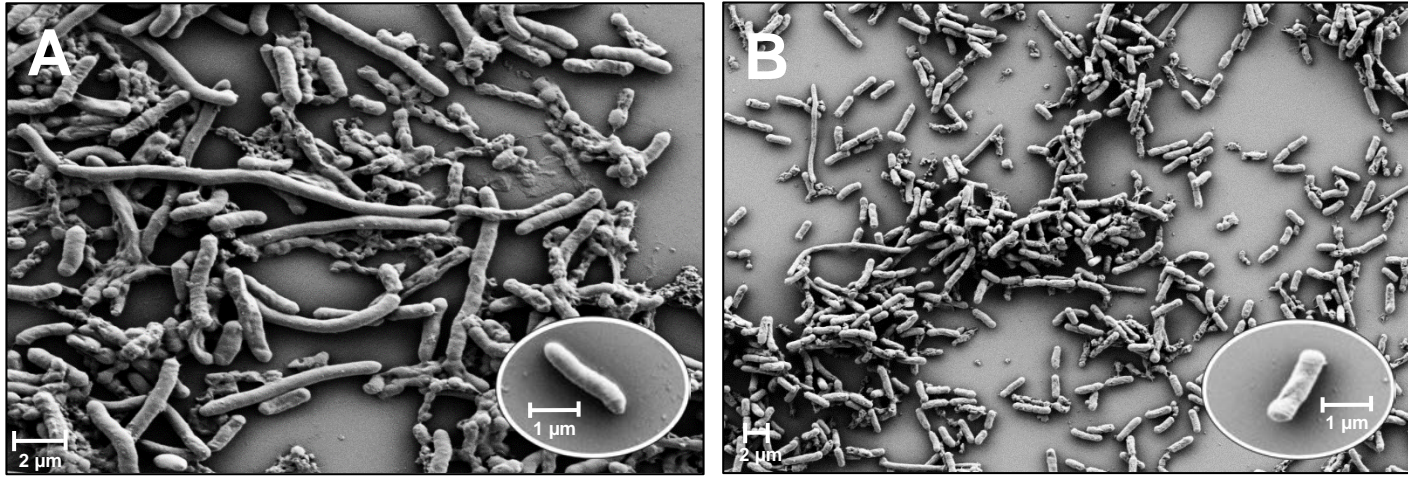


**Figure 4.** Microbial communities enriched from an aqueous sample collected on the southeast shore of Soap Lake (site SL2). Field Emission Scanning Electron Microscopy (FE-SEM) images of SL2 samples enriched under (A) facultative and (B) anaerobic conditions indicate the presence of numerous rod-shaped morphologies under both enrichment conditions.

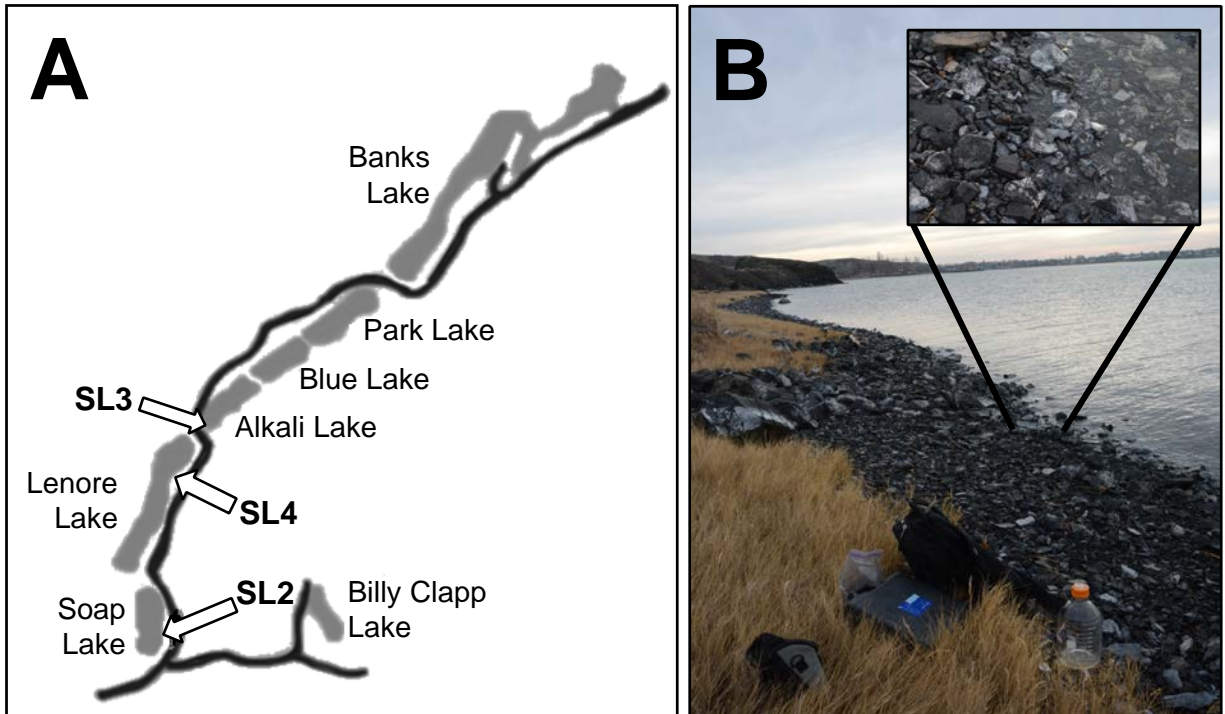


**Figure S1.** Soap Lake location and the sites selected for sample enrichment. The map (A) illustrates Soap Lake and surrounding areas with an arrow depicting the approximate location of sites SL2, SL3, and SL4 while images and inset (B) highlight the precise sampling location of site SL2.

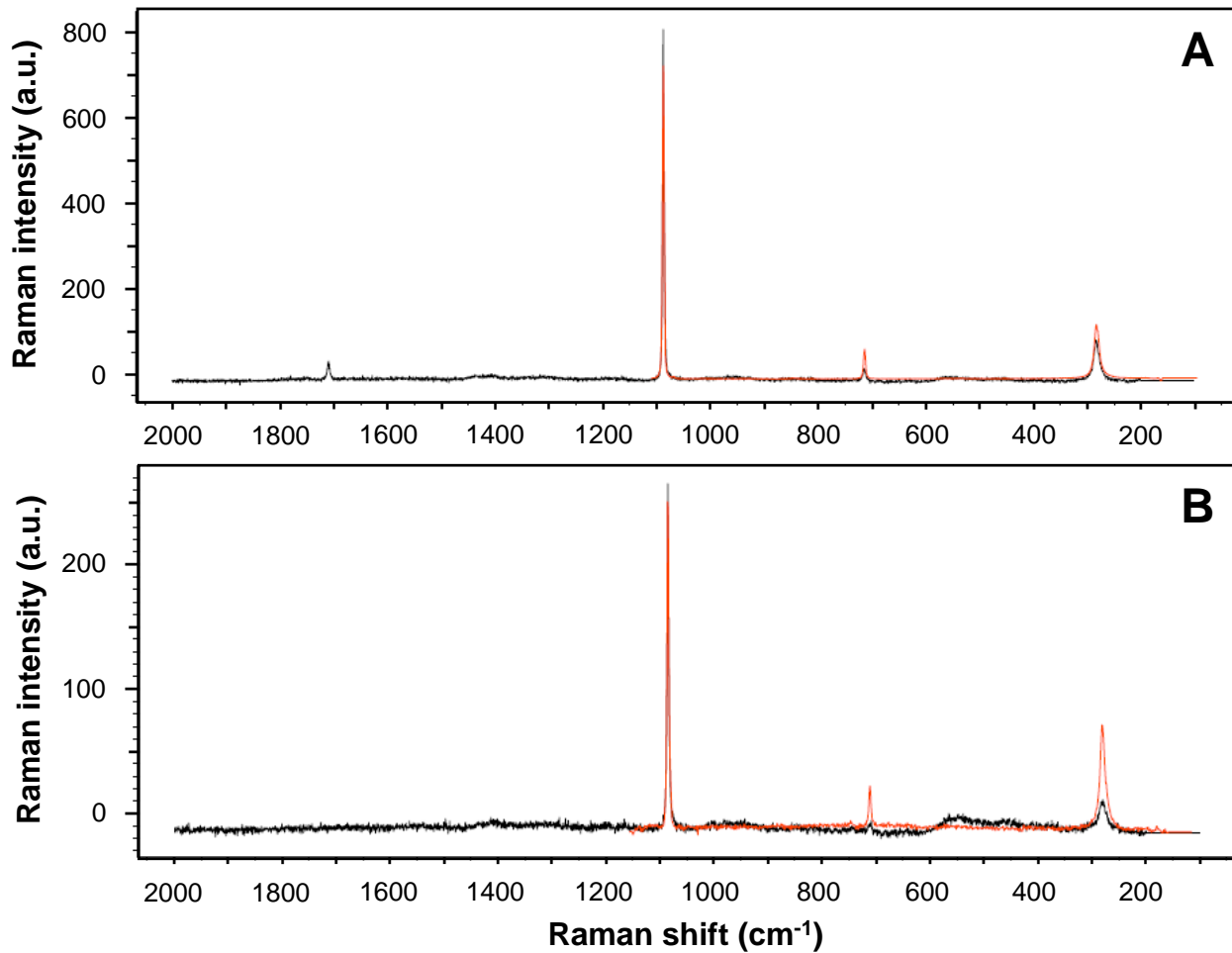


**Figure S2.** Raman spectra shown for mineral precipitates formed in facultative (A) and anaerobic (B) SL2 enrichments. A reference spectrum for calcite is displayed in orange while the acquired spectra are displayed in black.

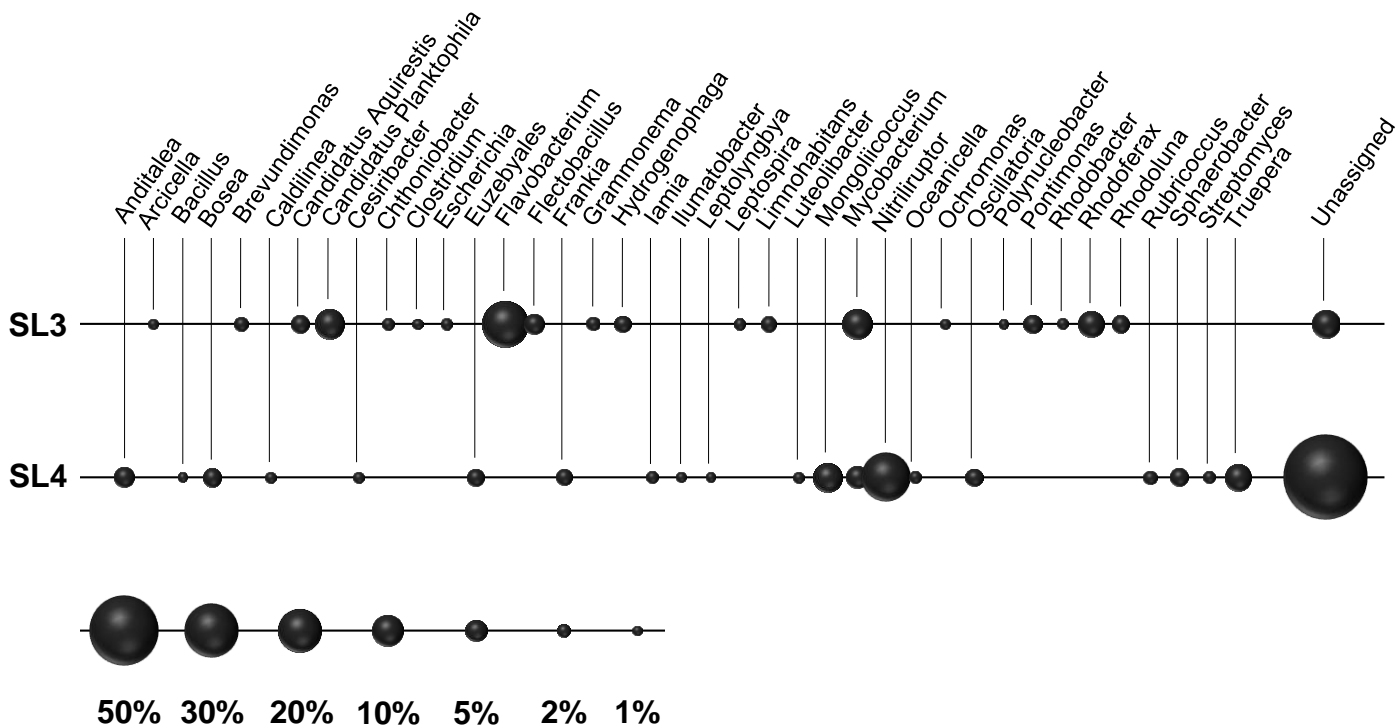


**Figure S3.** Relative abundance of major genus-level clades at two high pH and high salinity locations in the Soap Lake (WA) drainage. The relative abundance of a genus is proportional to the area of the circle, as depicted by the scale bar on the bottom. Only genera with a relative abundance  $\geq 1\%$  are shown.

**Table S1.** Aqueous Geochemistry

<b>Constituent</b>	<b>units</b>	<b>SL2</b>	<b>SL3</b>
pH		9.85	9.05
Temperature	°C	2.0	1.8
Conductivity	mV	-115.2	-75.2
Cl <sup>-</sup>	mmol l <sup>-1</sup>	57.7	0.7
F <sup>-</sup>	μmol l <sup>-1</sup>	419.1	88.7
NO <sub>3</sub> <sup>-</sup>	μmol l <sup>-1</sup>	116.2	35.6
SO <sub>4</sub> <sup>2-</sup>	mmol l <sup>-1</sup>	537.9	4.1
Ca	μmol l <sup>-1</sup>	62.4	405.2
Mg	mmol l <sup>-1</sup>	0.12	1.71
Na	mmol l <sup>-1</sup>	231.4	6.5
K	mmol l <sup>-1</sup>	13.1	0.7
Se	μmol l <sup>-1</sup>	64.1	0.8